Synthetic far-red light-mediated CRISPR-dCas9 device for inducing functional neuronal differentiation

Jiawei Shao[a,1], Meiyan Wang[a,1], Guiling Yu[a,1], Sucheng Zhu[a], Yuanhuan Yu[a], Boon Chin Heng[b], Jiali Wu[a], and Haifeng Ye[a,2]

[a]Synthetic Biology and Biomedical Engineering Laboratory, Shanghai Key Laboratory of Regulatory Biology, Institute of Biomedical Sciences and School of Life Sciences, East China Normal University, 200241 Shanghai, China; and [b]Faculty of Dentistry, The University of Hong Kong, Pokfulam, Hong Kong Special Administrative Region 999077, China

Edited by Sang Yup Lee, Korea Advanced Institute of Science and Technology, Daejeon, Republic of Korea, and approved June 12, 2018 (received for review February 9, 2018)

The ability to control the activity of CRISPR-dCas9 with precise spatiotemporal resolution will enable tight genome regulation of user-defined endogenous genes for studying the dynamics of transcriptional regulation. Optogenetic devices with minimal phototoxicity and the capacity for deep tissue penetration are extremely useful for precise spatiotemporal control of cellular behavior and for future clinic translational research. Therefore, capitalizing on synthetic biology and optogenetic design principles, we engineered a far-red light (FRL)-activated CRISPR-dCas9 effector (FACE) device that induces transcription of exogenous or endogenous genes in the presence of FRL stimulation. This versatile system provides a robust and convenient method for precise spatiotemporal control of endogenous gene expression and also has been demonstrated to mediate targeted epigenetic modulation, which can be utilized to efficiently promote differentiation of induced pluripotent stem cells into functional neurons by up-regulating a single neural transcription factor, *NEUROG2*. This FACE system might facilitate genetic/epigenetic reprogramming in basic biological research and regenerative medicine for future biomedical applications.

synthetic biology | optogenetics | far-red light | CRISPR-dCas9 | regenerative medicine

Complex cellular activities such as metabolism, circadian rhythm, and lineage-fate programming involve precise coordination of the dynamic transcriptional regulation of several genes at the same time. The proper functioning of complex transcriptional networks is therefore dependent on the precise regulation of endogenous gene expression. Recently, CRISPR-based systems have been developed as powerful tools for gene editing in diverse biological and therapeutic applications (1–7). These systems, consisting of a Cas9 nuclease and a single-guide RNA (sgRNA) targeting a specific gene, make it relatively easy to precisely regulate gene expression in a variety of biological processes, including gene silencing, genetic-defect compensation, and lineage-fate programming (8–13). Moreover, modifications to the CRISPR/Cas9 tool were recently developed as robust systems for in vivo activation of endogenous target genes through transepigenetic remodeling, with the objective of ameliorating disease phenotypes in mouse models of diabetes, acute kidney injury, and muscular dystrophy (14).

During development, precise spatiotemporal regulation of gene networks is of paramount importance. One possible approach to conditionally target and induce regulation of mammalian gene expression with high precision is the development of optogenetic transcriptional control systems based on dCas9, by incorporating light-responsive domains to enable dynamic regulation of endogenous gene activation with light (15–20). However, almost all existing CRISPR-Cas9–based photoactivatable transcription systems that are triggered by blue light (18, 20) exert relatively strong phototoxic effects on mammalian cells and also are limited by poor penetrative capacity through turbid human tissues (21). Moreover, specialized hardware and software are often required to deliver short pulses of high-frequency blue light over extended periods of illumination that may exceed 24 h to enable significant activation of these transcription systems, as reported in the literature (18, 20). This severely restricts the adoption of such photoactivatable systems for further translational research and clinical applications.

To overcome these limitations, we sought to develop an inducible light-responsive transcription system that would have low phototoxicity and background activity and which would also be fine-tunable, reversible, easy to implement, and can be widely applied. In our previous study, we developed a far-red light (FRL)-controlled transcription device based on the bacterial light-activated cyclic diguanylate monophosphate (c-di-GMP) synthase BphS and the c-di-GMP–responsive hybrid transactivator p65–VP64–NLS–BldD to regulate transgene expression (22). However, it can activate exogenous genes only in the presence of far-red light stimulation (22). In this study, we have designed and created a FRL-activated CRISPR-dCas9 effector (FACE) system based on dCas9 (23–25) and the bacterial phytochrome BphS (26), which enables transcriptional activation of user-defined exogenous or endogenous genes under FRL illumination with high induction efficiency and low background activity. With this FACE system we can also achieve in vivo activation of endogenous target genes through transepigenetic remodeling by FRL. In addition, this system is demonstrated to efficiently activate endogenous transcription factors that

Significance

We have developed an optogenetic far-red light (FRL)-activated CRISPR-dCas9 system (FACE) that is orthogonal, fine-tunable, reversible, and has robust endogenous gene-activation profiles upon stimulation with FRL, with deep tissue penetration capacity, low brightness, short illumination time, and negligible phototoxicity. The FACE device is biocompatible and meets the criteria for safe medical application in humans, providing a robust differentiation strategy for mass production of functional neural cells from induced pluripotent stem cells simply by utilizing a beam of FRL. This optogenetic device has expanded the optogenetic toolkit for precise mammalian genome engineering in many areas of basic and translational research that require precise spatiotemporal control of cellular behavior, which may in turn boost the clinical progress of optogenetics-based precision therapy.

Author contributions: H.Y. designed research; J.S., M.W., G.Y., S.Z., Y.Y., and J.W. performed research; J.S., M.W., G.Y., and H.Y. analyzed data; and J.S., M.W., G.Y., B.C.H., and H.Y. wrote the paper.

The authors declare no conflict of interest.

This article is a PNAS Direct Submission.

[1]J.S., M.W., and G.Y. contributed equally to this work.

[2]To whom correspondence should be addressed. Email: hfye@bio.ecnu.edu.cn.

This article contains supporting information online at www.pnas.org/lookup/suppl/doi:10.1073/pnas.1802448115/-/DCSupplemental.

can induce differentiation of neural-lineage cells from induced pluripotent stem cells (iPSCs). This system thus offers a versatile tool for many diverse applications that require dynamic regulation of gene expression or targeted epigenetic modifications, including the development of therapeutic interventions and the induction of cell differentiation.

Results

Design and Optimization of a FACE System. To create an efficient CRISPR-dCas9–based photoactivatable transcription system with low phototoxicity and deep tissue penetrative capacity, we constructed a FACE system (Fig. 1 *A*–*C*) based on a fully orthogonal FRL-triggered optogenetic system (22) in which the BphS is an FRL-activated c-di-GMP synthase (26, 27) and the transcription factor BldD is derived from *Streptomyces coelicolor* (28, 29) to achieve dynamic regulation of gene expression. The FRL-dependent hybrid transactivator p65–VP64–NLS–BldD could dimerize in the presence of c-di-GMP and bind to its chimeric promoter P_{FRL} to initiate downstream gene expression (Fig. 1*A*). These previous studies demonstrated that the synergistic activation mediator (SAM) system can be developed to enhance the efficiency of gene activation by engineering the sgRNA bearing MS2 RNA aptamers (23). By fusing MS2 proteins with various activators such as the 65-kDa transactivator subunit of NF-κB (p65) and heat shock factor 1 (HSF1) transactivation domains, sgRNA-mediated recruitment of a MS2–p65–HSF1 complex could improve the activation efficiency of dCas9-targeted endogenous genes. Therefore, we hypothesize that optical control of MS2-mediated recruitment of transcriptional activators might enable more potent transcriptional activation.

We first generated optogenetic transcriptional activation systems containing different variants of transactivators (FGTAx) by assembling MS2 fused to P65, VP64–p65–Rta (VPR), (12) or to HSF1 (Fig. 1*B*) recruited by sgRNAs bearing MS2 RNA aptamers, so as to assess the induction potency of genes targeted by dCas9-FGTAs. To obtain a robust light-inducible transcription system, we have constructed different transactivators (FGTAx) (Fig. 1*B*) and several FRL-responsive chimeric promoter variants (P_{FRLx}) (Fig. 1*C*), which were assembled into various configurations. Subsequently, we tested and identified which combination induces reporter gene expression most efficiently. We found that a combination of P_{FRL1a} and FGTA1 [P_{FRL3a}–FGTA1–pA (pGY48)] resulted in the most optimal FRL-triggered exogenous transcriptional responses (Fig. 1 *D*–*H*). Nevertheless, this combination did not exhibit very strong activation of endogenous achaete-scute homolog 1 (*ASCL1*) gene expression (~38-fold) in HEK293 cells (*SI Appendix*, Fig. S1). Hence, we speculate that the fusion transactivator FGTA1 (MS2–VP64) is not potent enough to up-regulate the required levels of endogenous gene expression, whereas the transcriptional activator FGTA4 (MS2–p65–HSF1) displayed significant activation potential (Fig. 1 *D*–*H*).

To improve robustness of the system, we further optimized the FACE system by testing the capacity of different variants of BldD-responsive promoters to up-regulate different amounts of the transcriptional activator FGTA4 with different FRL-specific promoters (P_{FRLx}) (Fig. 1 *I*–*K*). We found that HEK293 cells cotransfected with pWS46 (P_{hCMV}–BphS–P2A–YhjH–pA), pGY32 (P_{hCMV}–FRTA3–pA), pSZ69 (P_{hCMV}–dCas9–pA), pGY102 (P_{FRL1b}–FGTA4–pA), pWS137 [P_{U6}–sgRNA1 (P_{FACE})–pA], and pWS107 [P_{FACE}–human placental secreted alkaline phosphatase (SEAP)–pA] exhibited the highest fold FRL-triggered exogenous transgene activation (Fig. 1*K*). In addition, this configuration could efficiently activate endogenous gene expression (Fig. 1*L*).

Characterization of the Optimized FACE System. The detailed performance of the FACE system was further characterized. To assess the impact of FRL (730 nm) and blue light (465 nm) on the metabolic integrity and viability of mammalian cells, HEK293 cells were transfected with pSEAP2-control and then were exposed to light for 48 h, followed by quantification of SEAP expression levels and cell viability (*SI Appendix*, Fig. S2 *A* and *B*). The control experiment data demonstrated that FRL is minimally phototoxic to mammalian cells compared with blue light (*SI Appendix*, Fig. S2 *A* and *B*). The different wavelengths of light-triggered transgene expression of the FACE system suggest that this optogenetic tool exhibited the best SEAP induction ratios under FRL (730 nm) illumination, thus indicating the chromatic specificity of the FACE device (*SI Appendix*, Fig. S3). We further characterized the detailed performance of the transgene expression kinetics of the FACE device. The data showed that the transgene expression triggered by FRL was illumination intensity- and exposure time-dependent (Fig. 2 *A* and *B*). We then transduced the FACE device into different cell lines and found that it was functional in a number of mammalian cell types (Fig. 2*C*), demonstrating the applicability and compatibility of this photoactivatable transcription system in a broad range of applications. The variable transcriptional performance of the FACE device in different mammalian cells lines could probably be due to the different transfection efficiencies as well as potential interactions with endogenous cell components of different cell lines. Moreover, the FACE system was demonstrated to exhibit fully reversible transcription activation kinetics (Fig. 2*D*) and precise spatiotemporal transgene activation (Fig. 2 *E* and *F*).

Photoactivation of User-Defined Endogenous Genes with the FACE System. To test whether the FACE system could control endogenous gene activation, we activated the endogenous gene target by delivering the FACE system with a group of two sgRNAs that target the promoter region of the human *ASCL1* gene into HEK293 cells. We then used qRT-PCR to assess the activation of *ASCL1* gene after 6 h of FRL illumination or in the dark and found that *ASCL1* was successfully up-regulated using each sgRNA, with significant further enhancement upon using two mixed sgRNAs compared with a single sgRNA (*SI Appendix*, Fig. S4). It was notable that mixed sgRNAs transfection did not affect *ASCL1* expression in the dark but resulted in high levels of induction by FRL. These results further demonstrated that our FACE system could induce endogenous gene expression by FRL and produce a high level of transcriptional activation with mixed sgRNAs. The detailed performance of the endogenous gene activation kinetics using the FACE system was further characterized. The data showed that the endogenous *ASCL1* up-regulation triggered by FRL was illumination intensity- and exposure time-dependent (Fig. 3 *A* and *B*). We further confirmed that the FACE system was able to robustly activate endogenous *ASCL1* expression in different mammalian cell lines (Fig. 3*C*), further indicating that the FACE system has broad utility for a wide range of applications.

In addition to sustaining gene activation, it is also important to have the capacity to regulate gene expression reversibly in some biological processes that exhibit temporal gene-expression patterns. We therefore tested whether endogenous gene activation by the FACE system is reversible by investigating the switch-on and switch-off kinetics of FRL-induced *ASCL1* up-regulation by the FACE device (Fig. 3*D*). The transfected cells were illuminated with FRL for the first 20 min, and the *ASCL1* mRNA level was sustainably up-regulated in the following 12 h but subsequently decreased to baseline level within 24 h. When the same batch of cells was exposed to FRL for another 20 min after 48 h of incubation, the *ASCL1* mRNA level could be up-regulated again (Fig. 3*D*). Collectively, these results demonstrated that the FACE system could reversibly activate endogenous gene expression.

Additionally, we sought to investigate whether this system could be applied to induce multiple endogenous gene transcription. We therefore generated four pairs of sgRNAs with each pair targeting the promoters of titin (*TTN*), interleukin 1 receptor antagonist

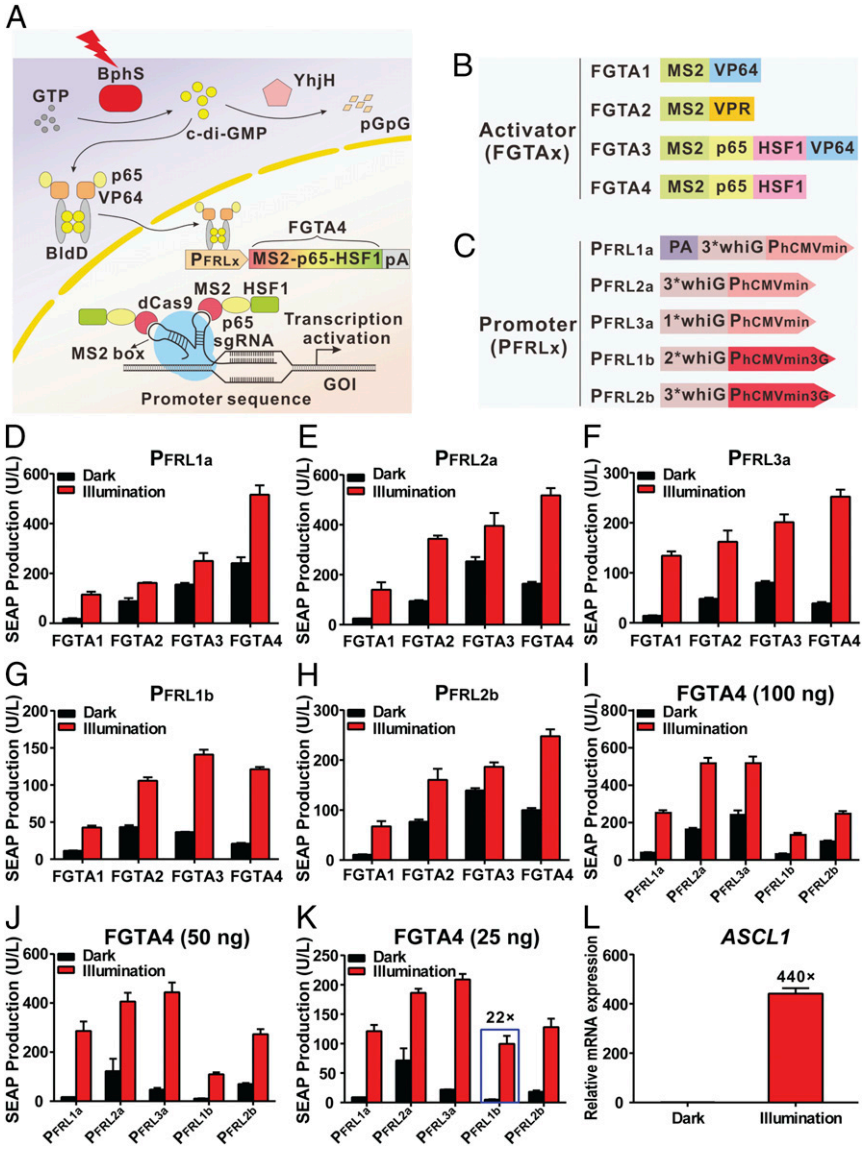

Fig. 1. Design and optimization of the FACE system. (*A*) Schematic representation of the FACE system. The engineered bacterial photoreceptor BphS is activated by FRL (~730 nm) to convert GTP into c-di-GMP. Increased cytosolic c-di-GMP production dimerizes the FRL-dependent transactivator p65–VP64–NLS–BldD, enabling it to bind to its chimeric promoter P_{FRLx} to initiate expression of the FRL-inducible genome transactivator (FGTA4) by assembling MS2, p65, and HSF1 into different protein configurations which are further recruited by the MS2 box of the sgRNA–dCas9 complex to induce transgene expression. (*B*) Different configurations of the FRL-inducible genome transactivators (FGTAx). (*C*) Different configurations of the FRL-inducible genome promoters P_{FRLx}. (*D–H*) Optimization of the P_{FRLx}-driven FGTAx expression vector variants for the FACE system. HEK293 cells (6×10^4) were cotransfected with pWS46 (P_{hCMV}–BphS–2A–YhjH–pA), pGY32 (P_{hCMV}–FRTA3–pA), pSZ69 (P_{hCMV}–dCas9–pA), pWS137 [P_{U6}–sgRNA1 (P_{FACE})–pA], and pWS107 (P_{FACE}–SEAP–pA) and with P_{FRL1a} [pA–$(whiG)_3$–$P_{hCMVmin}$] (*D*), P_{FRL2a} [$(whiG)_3$–$P_{hCMVmin}$] (*E*), P_{FRL3a} [(whiG)–$P_{hCMVmin}$] (*F*), P_{FRL1b} [$(whiG)_2$–$P_{hCMVmin3G}$] (*G*) or P_{FRL2b} [$(whiG)_3$–$P_{hCMVmin3G}$] (*H*)–driven FGTA1 (pGY50, pGY49, pGY48, pGY99, and pGY74) or with FGTA2 (pGY53, pGY52, pGY51, pGY100, and pGY75) or FGTA3 (pGY56, pGY55, pGY54, pGY101, and pGY76) or FGTA4 (pGY59, pGY58, pGY57, pGY102, and pGY77) at a 2:2:1:1:1:2 ratio (wt/wt/wt/wt/wt/wt) and then were illuminated with FRL (1.5 mW/cm^2, 730 nm) for 6 h daily. SEAP expression in the culture supernatants was assayed at 48 h after the first illumination. (*I–K*) Optimization of FRL-specific promoter (P_{FRLx})-driven FGTA2.4 (MS2–p65–HSF1) for the FACE system. HEK293 cells (6×10^4) were cotransfected with 100 ng pWS46, 100 ng pGY32, 50 ng pWS137, 50 ng pWS107, and 50 ng pSZ69 and with 100 ng (*I*), 50 ng (*J*), or 25 ng (*K*) of the expression vector variants pGY59 [P_{FRL1a}: pA–$(whiG)_3$–$P_{hCMVmin}$], pGY58 [P_{FRL2a}: $(whiG)_3$–$P_{hCMVmin}$], pGY57 [P_{FRL3a}: (whiG)–$P_{hCMVmin}$], pGY102 [P_{FRL1b}: $(whiG)_2$–$P_{hCMVmin3G}$], or pGY77 [P_{FRL2b}: $(whiG)_3$–$P_{hCMVmin3G}$]-driven FGTA4 (MS2–p65–HSF1) and then were illuminated for 6 h with FRL (1.5 mW/cm^2, 730 nm) daily. SEAP expression in the culture supernatants was assayed at 48 h after the first illumination. The blue frame in *K* marks the best-in-class condition chosen for the subsequent experiments. All data are expressed as means ± SD; $n = 3$ independent replicate experiments in *D–K*. (*L*) Activation of the endogenous *ASCL1* gene by targeting sgRNAs under FRL illumination with the FACE system. HEK293 cells (6×10^4) were cotransfected with pWS46, pGY32, pSZ83 [P_{U6}–sgRNA1 (*ASCL1*)–pA], pSZ84 [P_{U6}–sgRNA2 (*ASCL1*)–pA], pSZ69, and pGY102 at a 4:4:2:2:2:1 ratio (wt/wt/wt/wt/wt/wt) and then were illuminated with FRL (1.5 mW/cm^2, 730 nm) for 6 h daily. At 48 h after the first illumination, relative mRNA expression levels compared with that in the dark were quantified by qRT-PCR and are presented as means ± SD; $n = 3$ independent replicate experiments.

(*IL1RN*), *ASCL1*, and rhox homeobox family member 2 (*RHOXF2*) and tested the FRL-induced endogenous gene transcription system in HEK293 cells. The qRT-PCR results showed that the FACE system could achieve optogenetic control of multiplexed endogenous gene transcription in the genome without affecting the others (Fig. 3*E*), thus demonstrating simultaneous activation of user-defined endogenous gene(s) of interest with the FACE system.

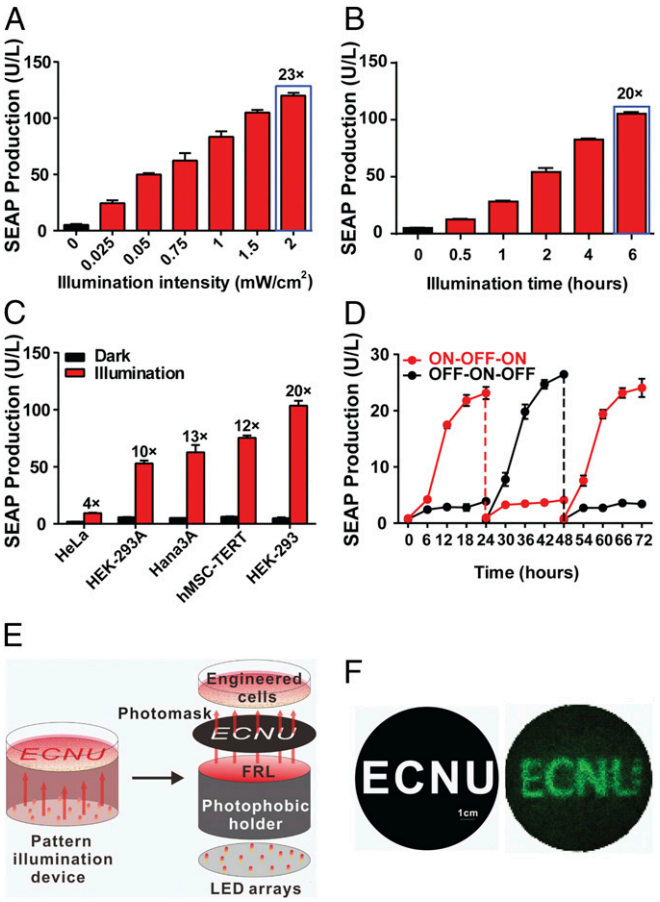

Fig. 2. Characterization of the FACE system. (*A*) Illumination-dependent FACE system activity. HEK293 cells were cotransfected with pWS46, pGY32, pGY102, pSZ69, pWS137, and pWS107 at a 4:4:1:2:2:2 (wt/wt/wt/wt/wt/wt) ratio and were illuminated with FRL at different light intensities (0–2 mW/cm^2) for 6 h daily. SEAP expression was quantified in the culture supernatant 48 h after the first illumination. (*B*) Exposure time–dependent FACE system activity. HEK293 cells were cotransfected as described in *A* and were illuminated with FRL (1.5 mW/cm^2) for different periods of time every day. SEAP expression was assessed in the cell-culture supernatant at 48 h after the first illumination. (*C*) FACE–induced SEAP expression in different mammalian cell lines. Different mammalian cell lines were cotransfected as described in *A* and were exposed to FRL (1.5 mW/cm^2; 730 nm) for 6 h every day. SEAP expression in the culture supernatant was assayed at 48 h after the first illumination. (*D*) Reversibility of the FACE-triggered transgene expression. HEK293 cells cotransfected as described in *A* were either kept in the dark (OFF) or were illuminated with FRL (1.5 mW/cm^2) for 20 min (ON), and SEAP production was quantified every 6 h for 72 h. The culture medium was refreshed every 24 h with concomitant reversal of illumination status. All data are expressed as means ± SD; $n = 3$ independent replicate experiments. (*E*) Setup for pattern illumination. The far-red LEDs were mounted on the bottom of a photophobic holder, and an ECNU-patterned mask made from aluminum foil was placed on top of the photophobic holder to illuminate tissue-culture dishes up to 10 cm in diameter. In this setup, the pattern on the photomask can be projected onto the bottom of the tissue-culture dish by FRL. (*F*) Spatial control of FRL-dependent transgene expression mediated by the FACE system. HEK293 cells cotransfected with pWS46, pGY32, pGY102, pSZ69, pWS137, and pGY47 at a 4:4:1:2:2:2 (wt/wt/wt/wt/wt/wt) ratio were illuminated (1.5 mW/cm^2, 730 nm) for 6 h through the photomask (*Left*), resulting in a corresponding pattern of EGFP expression (*Right*).

Photoactivation of Endogenous Genes with the FACE System in Mice. To demonstrate the superiority of the FACE system in vivo, we investigated the activation of endogenous target genes in mice with this system. First, we compared the endogenous gene-activation efficiency of the FRL-controlled FACE system and the blue light-controlled system (CPTS 2.0) (20) in vivo. Optogenetically engineered cells seeded in hollow fibers were implanted into the dorsum of mice and exposed to FRL or blue light for 2 h (5 mW/cm^2) (Fig. 4*A*). As shown by the data (Fig. 4*B*), our FACE system demonstrated very efficient endogenous gene *ASCL1* up-regulation of about 195-fold compared with mice in the dark. This is mainly due to deep penetration by FRL. In contrast, the CPTS 2.0 blue light-controlled system showed only ninefold *ASCL1* up-regulation. We then further examined whether the FACE system could be used to modulate the in vivo activation of endogenous target genes through transepigenetic remodeling. This study focused on endogenous genes involved in muscle mass and regeneration in an attempt to treat several myopathies or muscle loss associated with chronic diseases. We targeted the mouse laminin subunit alpha 1 (*Lama1*) gene or follistatin (*Fst*) gene because increased expression of *Lama1* could provide new mechanical linkages between the extracellular matrix and the sarcolemma (30), while overexpressed *Fst* could increase muscle mass (14). The tibialis posterior muscles of the mice were electroporated with a total of 40 μg of the plasmids containing the FACE system or the CPTS 2.0 system with a group of two sgRNAs that specifically target the promoter regions of the *Lama1* or *Fst* genes. This was followed by illumination with FRL or blue light (10 mW/cm^2) for 4 h each day (Fig. 4*C*). The qPCR results showed that the endogenous *Lama1* (Fig. 4*D*) or *Fst* (Fig. 4*E*) gene was significantly up-regulated by the FACE system (approximately twofold for *Lama1* and approximately fivefold for *Fst*, compared with mice in the dark). However, CPTS2.0 did not up-regulate *Lama1* or *Fst* gene expression in muscle tissues compared with mice in the dark. Collectively, these data indicate that the FACE system might be used for targeting epigenetic modifications and further confirm that the FACE system is much superior to the previously reported CPTS 2.0 blue light-inducible system, particularly for in vivo applications.

Optogenetic Control of Neuronal Differentiation of iPSCs with the FACE System. Despite great potential, the generation of functional neurons from iPSCs for transplantation is limited in clinical applications due to the long duration of culture required for neural induction and the low efficiency of neural-lineage differentiation. Much ongoing effort has been focused on optimizing culture protocols to enhance neural-lineage differentiation from stem cells (31, 32).The ability to selectively up-regulate gene expression provides another promising strategy to direct somatic or stem cell differentiation for regenerative medicine applications. Previous studies have shown that ectopic expression of neurogenin 2 (*NEUROG2*) or neurogenic differentiation factor 1 (*NEUROD1*) is sufficient to induce neuronal differentiation from iPSCs (33–35). Therefore, in this study, we tested whether the FACE system with sgRNAs targeting *NEUROG2* could optogenetically initiate functional neural differentiation from mouse iPSCs (Fig. 5*A*). Firstly, we optimized and confirmed that iPSCs transfected with the FACE system without YhjH exhibited brighter EGFP fluorescence intensity under FRL illumination than cells incubated in the dark (*SI Appendix*, Fig. S5). Next, we generated stable iPSCs lines integrated with the FACE system, which were then transduced with lentiviral vectors containing a mixed pool of two sgRNAs that target *NEUROG2*. To confirm the efficiency of neural-lineage differentiation, the stable iPSC cell lines containing sgRNAs were exposed to FRL and were closely monitored for biochemical and phenotypic changes. qRT-PCR analysis revealed that the *NEUROG2* mRNA expression level was significantly up-regulated in the illuminated cells compared with cells in the dark (Fig. 5*B*). We also observed that the stable iPSCs exhibited typical morphological features of a neuronal cell under FRL illumination (Fig. 5*C*). In addition, these cells stained positively for the neuronal markers neurofilament 200 and beta III tubulin (Tuj1) after 8 d of FRL illumination (Fig. 5*C*). Moreover, the expression of

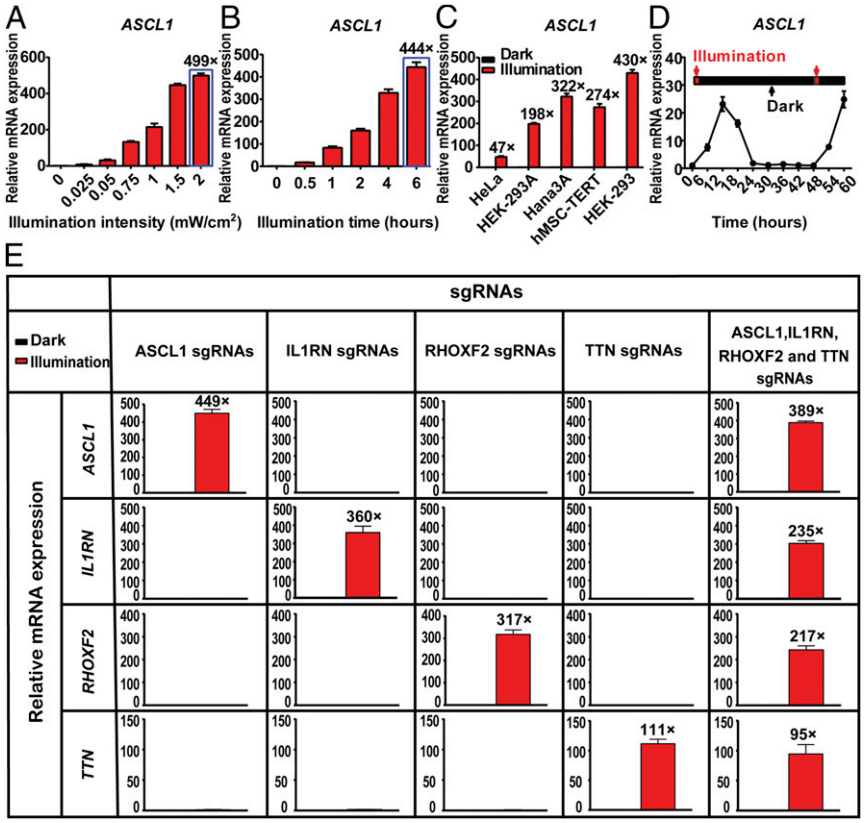

Fig. 3. FRL-inducible, RNA-guided activation of endogenous genes by the FACE system. (*A*) Illumination-dependent FACE-induced endogenous *ASCL1* expression. HEK293 cells were cotransfected with pWS46, pGY32, pGY102, pSZ69, pSZ83, and pSZ84 at a 4:4:1:2:2:2 (wt/wt/wt/wt/wt/wt) ratio, followed by illumination with FRL at different light intensities (0–2 mW/cm^2) for 6 h daily. (*B*) Exposure time-dependent FACE-induced endogenous *ASCL1* expression. HEK293 cells were cotransfected as described in *A* and were illuminated with FRL (1.5 mW/cm^2) for different time periods every day. (*C*) FACE-induced endogenous *ASCL1* expression in different mammalian cell lines. Different mammalian cell lines were cotransfected as described in *A* and were exposed to FRL (1.5 mW/cm^2; 730 nm) for 6 h every 24 h. (*D*) Reversibility of the FACE-induced endogenous *ASCL1* expression. HEK293 cells were cotransfected as described in A, were illuminated with FRL (1.5 mW/cm^2) for 20 min, and then were kept in the dark. After 48 h of incubation, the cells were exposed to FRL for another 20 min. The endogenous *ASCL1* levels were quantified by qRT-PCR every 6 h. (*E*) Multiplexed endogenous gene activation in HEK293 cells containing the FACE system and the indicated sgRNAs. HEK293 cells were cotransfected with pWS46, pGY32, pGY102, and pSZ69 and with the corresponding sgRNAs: pSZ83 and pSZ84 or pSZ92 [P_{U6}–sgRNA1 (*IL1RN*)–pA] and pSZ93 [P_{U6}–sgRNA2 (*IL1RN*)–pA] or pSZ105 [P_{U6}–sgRNA1 (*RHOXF2*)–pA] and pSZ106 [P_{U6}–sgRNA2 (*RHOXF2*)–pA] or pSZ107 [P_{U6}–sgRNA1 (*TTN*)–pA] and pSZ108 [P_{U6}–sgRNA2 (*TTN*)–pA] or all eight mixed sgRNAs, followed by exposure to FRL (1.5 mW/cm^2; 730 nm) for 6 h every day. The data are expressed as relative mRNA expression levels quantified by qRT-PCR at 48 h after the first illumination. All data are presented as the mean ± SD (n = 3 independent replicate platings of each culture).

typical neural-lineage markers including *Sox1*, *Pax6*, *N-cadherin*, *Tuj1*, and *Nestin* was significantly up-regulated in the illuminated cells compared with cells in the dark (Fig. 5*D*). Finally, to further verify the functionality of the FRL-induced neuronal cells, calcium ion imaging was performed to monitor neuronal activity in the generated neurons in vitro. The results showed that the differentiated neuronal cells displayed a significant change in the calcium ion concentration within the cytosol upon treatment with 50 mM KCl (Fig. 5*E*). In conclusion, we can easily obtain functional neurons from iPSCs by FRL illumination with the FACE system.

Discussion

An ideal optogenetic CRISPR-dCas9 system would be orthogonal and provide fine-tunable and robust transcriptional control of selected genes in response to light with deep tissue penetration, low brightness, short illumination time, negligible phototoxicity, and excellent biocompatibility. In this study, we report the engineering of a light-controllable transcriptional activation system. Our FACE system can sufficiently activate high induction ratios of endogenous genes with continuous illumination at mild exposure strength (4–6 h, 0–2 mW/cm^2). This should be better tolerated by mammalian systems than the previously reported blue light-inducible system with repetitive short pulses of illumination over several days (18, 20, 36). The FACE system developed in this study is biocompatible and meets the criteria for safe medical applications in humans.

This FACE system is easily programmable, which provides a straightforward and robust method to regulate the simultaneous activation of user-defined endogenous multiplex genes with precise spatiotemporal control. Our system exhibits high induction efficiency upon illumination in various human cell lines with reasonably low background activity in the dark. Therefore this may be a suitable option if gene regulation with high temporal resolution is required to regulate endogenous gene expression precisely.

It should be possible to apply our FACE system to control gene transcriptional regulation in vivo, as light of wavelengths >600 nm is able to propagate further into tissues more efficiently than blue light (37). Compared with the blue light-controlled endogenous gene activation system (20), our FACE system can robustly trigger endogenous gene activation in mice, indicating many potential applications in vivo. Therefore, the FACE system developed in this study can pave the way for optogenetics-based translational research, and we anticipate that this system holds great promise

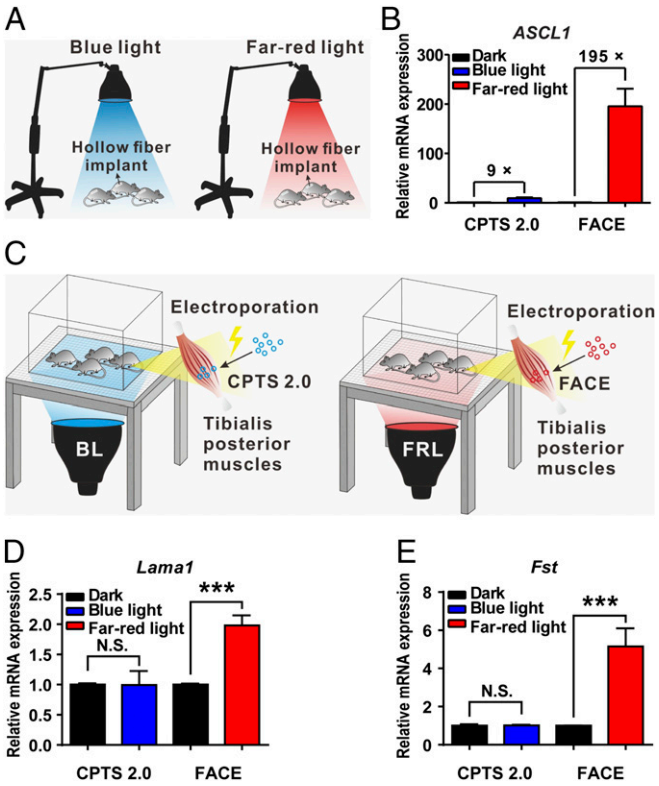

Fig. 4. A comparison of endogenous gene photoactivation with the CPTS 2.0 and the FACE system in mice. (*A*) A schematic of the experimental setup. The physiotherapy lamps were used for illumination of mice harboring transgenic implants under blue light or FRL. (*B*) Light-induced activation of *ASCL1* with the CPTS 2.0 blue light-inducible system and the FACE system in mice. Pairs of 2.5-cm hollow fibers containing a total of 2×10^6 pWS303 (P_{hCMV}–MS2–NES–CIBN–pA)/pWS304(P_{hCMV}–CRY2PHR–NLS–p65–HSF1–pA)/pSZ69/pSZ84/pSZ83 (CPTS 2.0) or pWS46/pGY32/pGY102/pSZ69/pSZ84/pSZ83 (FACE system) transgenic HEK293 cells were s.c. implanted into the dorsum of wild-type mice, and the mice were exposed to either blue light or FRL (5 mW/cm^2) for 2 h every day. The HEK293 cells were then collected from the hollow fibers, and the relative mRNA expression levels compared with that in the dark were quantified by qRT-PCR at 48 h after implantation. Data are expressed as mean ± SEM; $n = 5$ mice. (*C*) A schematic illustration of the experimental setup. The tibialis posterior muscles of the wild-type mice were electroporated with the CPTS 2.0 or the FACE system, and the mice were then illuminated from the bottom by blue light or FRL, respectively. (*D*) Light-induced activation of the endogenous *Lama1* gene with the CPTS 2.0 and FACE system in mice. The tibialis posterior muscles of the mice were electroporated with 40 μg of pWS303/pWS304/pGY174[P_{U6}–sgRNA1(*Lama1*)–pA–P_{U6}–sgRNA2(*Lama1*)–pA–P_{hCMV}–dCas9–pA] (CPTS2.0) or pWS46/pGY32/pGY102/pGY174 (FACE system) plasmids, and the mice were exposed to either blue light or FRL (10 mW/cm^2) for 4 h each day. Muscles were collected at 3 d after electroporation, and the relative mRNA expression levels compared with those in the dark were quantified by qRT-PCR. (*E*) Light-induced activation of the endogenous *Fst* gene with the CPTS 2.0 and FACE system in mice. The tibialis posterior muscles of the mice were electroporated with 40 μg of pWS303/pWS304/pGY177 [P_{U6}–sgRNA1(*Fst*)–pA–P_{U6}–sgRNA2(*Fst*)–pA–P_{hCMV}–dCas9–pA] (CPTS2.0) or pWS46/pGY32/pGY102/pGY177 (FACE system) plasmids, and the mice were exposed to either blue light or FRL (10 mW/cm^2) for 4 h each day. Muscle tissues were collected 3 d after electroporation, and the relative mRNA expression levels compared with those in the dark were quantified by qRT-PCR. The data in *D* and *E* are presented as the mean ± SEM; statistical analysis was by the two-tailed *t* test; $n = 5$ mice. ***$P < 0.001$ vs. control. N.S., not significantly different.

for a broad array of in vivo biomedical research applications in the future.

Conditional dCas9-based methodologies have broad applications in diverse biomedical fields (38, 39). For instance, inducible systems can be used to investigate embryonic development or stem cell differentiation and dissect the dynamic regulatory network orchestrating vertebrate development. Our FACE system also provides a robust method for generating functional neural cells from iPSCs under FRL illumination through the up-regulation of a single neural transcription factor. We anticipate that our FACE system with characteristics of reversible, tunable, spatiotemporal control of endogenous gene expression could expand the optogenetic toolkit for precise mammalian genome engineering in many areas of basic and translational research that require precise spatiotemporal control of cellular behavior, in turn boosting the clinical progress of precision optogenetics-based therapy.

Materials and Methods

Construction of Plasmids. Comprehensive design and construction details for all expression vectors are provided in *SI Appendix*, Table S1. Some plasmids were cloned by Gibson assembly according to the manufacturer's instructions [Seamless Assembly Cloning Kit; catalog no. BACR(C) 20144001; Obio Technology, Inc.]. All genetic components have been validated by sequencing (Genewiz, Inc.).

Cell Culture and Transfection. HEK293 cells (CRL-11268; ATCC), HEK293–derived HEK293A cells containing a stably integrated copy of the E1 gene (R70507; Thermo Fisher), HeLa (human cervical adenocarcinoma) cells (CCL-2; ATCC), telomerase-immortalized human mesenchymal stem cells (hMSC-TERT) (40), and HEK293-derived Hana3A cells engineered for constitutive expression of RTP1, RTP2, REEP1, and Gαoλϕ (41) were cultured in DMEM (catalog. no. 31600-083; Gibco) supplemented with 10% (vol/vol) FBS (catalog no. 04-001-1C; Biological Industries) and 1% (vol/vol) penicillin/streptomycin solution (catalog. no. L0022-100; Biowest). All cell types were cultured at 37 °C in a humidified atmosphere containing 5% CO_2 and were regularly tested for the absence of *Mycoplasma* and bacterial contamination. All cell lines were transfected with an optimized polyethyleneimine (PEI)-based protocol (42). Briefly, 6×10^4 cells per well were plated in a 24-well plate at 18 h before transfection and were subsequently incubated for 6 h with 50 μL of a 3:1 PEI DNA mixture (wt/wt) (PEI, molecular weight 40,000, stock solution 1 mg/mL in ddH_2O; catalog. no. 24765; Polysciences) containing 0.375 μg of plasmid DNA (total plasmid amount for FACE). Cell titers and viability were quantified with a Countess II automated cell counter (Life Technologies).

FRL-Controlled Gene Activation in Mammalian Cells. For exogenous gene-activation experiments, 6×10^4 cells were plated in a 24-well plate and were cultured for 18 h. The cells were transfected with 50 μL of a 3:1 PEI:DNA mixture (wt/wt) containing 0.375 μg of plasmid DNA (total plasmids amount for FACE). At 24 h after transfection, cells were illuminated for different time periods (0–6 h) or with different light intensities (0–2 mW/cm^2) using a custom-designed 4 × 6 far-red light LED array (730 nm; Epistar) (22). The light intensity was measured at a wavelength of 730 nm using an optical power meter (Q8230; Advantest) according to the manufacturer's operating specifications. SEAP expression levels in the culture medium were quantified at 48 h after transfection (*SI Appendix*, Fig. S6). For endogenous gene-activation experiments, HEK293 cells were cotransfected with 100 ng pWS46 (P_{hCMV}–BphS–2A–YhjH–pA); 100 ng pGY32 (P_{hCMV}–FRTA3–pA; FRTA3: p65–VP64–NLS–BldD); 25 ng pGY102 (P_{FRL1b}–FGTA4–pA; P_{FRL1b}: $(whiG)_2$–$P_{hCMVmin3G}$; FGTA4: MS2–P65–HSF1); 50 ng pSZ69 (P_{hCMV}–dCas9–pA), and 50 ng of the corresponding sgRNAs (*SI Appendix*, Table S3). The transfected cells were cultured for 24 h after transfection. The culture plates were then placed below a custom-designed 4 × 6 LED array. Each plate (maintained at 37 °C and 5% CO_2) was illuminated (1.5 mW/cm^2; 730 nm) for 6 h, once daily, for 2 d (*SI Appendix*, Fig. S6). The cells were harvested, and total RNA was extracted for qPCR analysis at 48 h after the first illumination.

Spatial Control of FRL-Dependent Gene Activation in Mammalian Cells. HEK293 cells (3×10^6) were plated into a 10-cm dish, cultured for 18 h, and transfected with 1,500 μL of a 3:1 PEI:DNA mixture (wt/wt) containing 11.25 μg of plasmid DNA (total plasmid amount for FACE). At 24 h after transfection, cells were illuminated for 6 h each day by FRL (1.5 mW/cm^2, 730 nm) with a photomask with the pattern "ECNU" made from aluminum foil. The patterned photomask was placed between the upward-facing LED array and the bottom of the 10-cm culture dish (Fig. 2*E*). Fluorescence images were acquired at 48 h after illumination using ChemiScope 4300 Pro imaging equipment (Clinx).

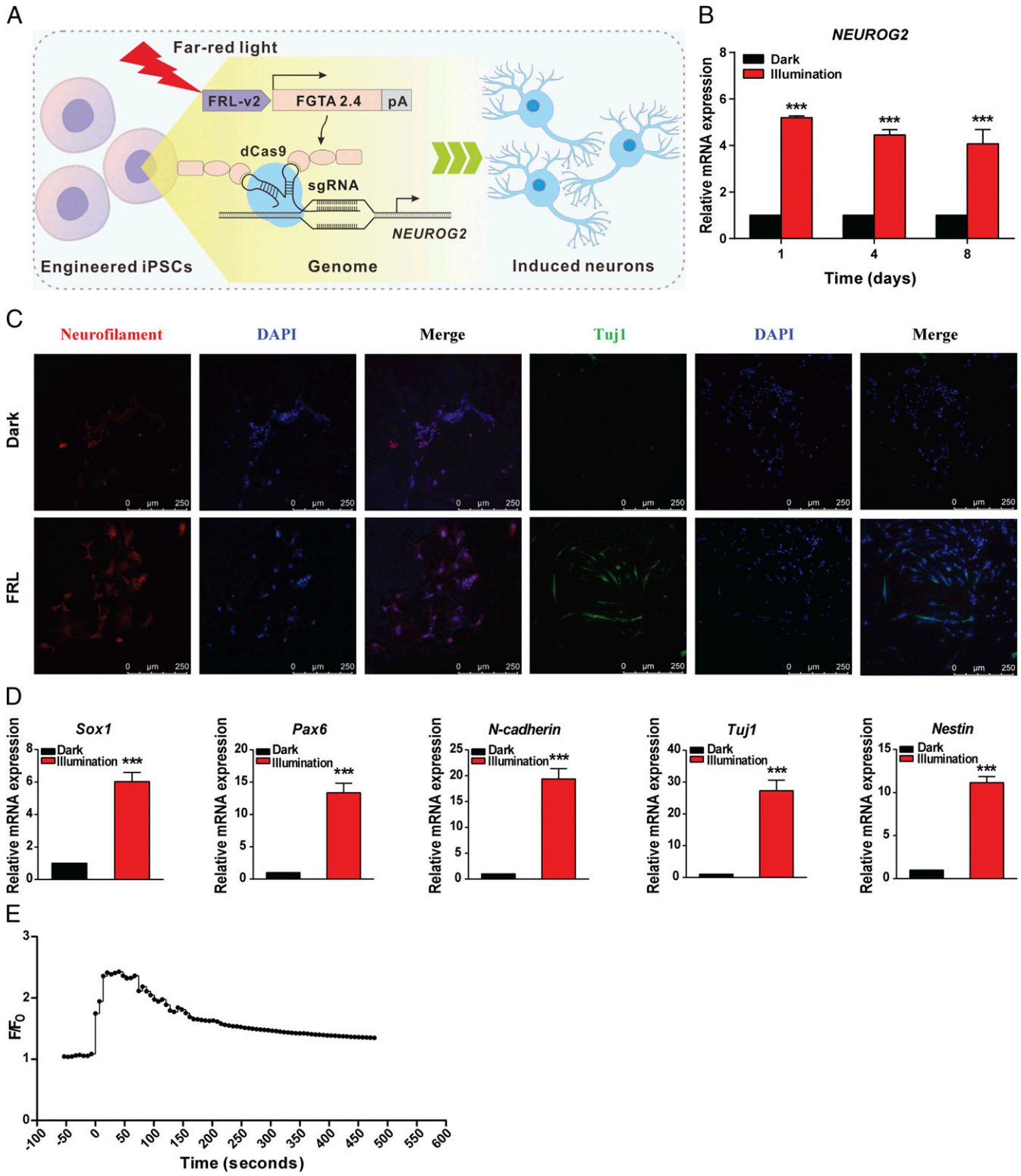

Fig. 5. FRL-stimulated iPSCs differentiate into functional neurons with the FACE system. (*A*) Schematic representation of FRL-induced neuronal differentiation from iPSCs with the FACE system. (*B*) FRL-induced *NEUROG2* up-regulation in iPSCs with the FACE system and two sgRNAs targeting *NEUROG2* after 1, 4, and 8 d of FRL illumination for 6 h every day or incubation in the dark. Relative mRNA expression levels compared with those in the dark were quantified by qRT-PCR and are presented as means ± SD; $n = 3$ independent replicate experiments; ***$P < 0.001$. (*C*) Immunofluorescence images of iPSCs showing the positive expression of neuronal markers neurofilament (magenta) and Tuj1 (green) after 8 d of FRL illumination for 6 h every day. Cell nuclei were counterstained with DAPI (blue). Stable iPSC lines containing the FACE system were transduced with lentiviral preparations containing two sgRNAs targeting *NEUROG2*. The images are representative of at least three replicate experiments. (Scale bars, 250 μm.) (*D*) qRT-PCR analysis of mRNA expression levels of neuronal marker genes (*Sox1*, *Pax6*, *N-cadherin*, *Tuj1*, and *Nestin*) by iPSC lines after 8 d of FRL illumination. All data are presented as the mean ± SD; $n = 3$ independent replicate experiments. ***$P < 0.001$. (*E*) Calcium ion imaging analysis of FRL-induced neurons by Fluo-4 AM. The iPSC-derived functional neurons treated with 50 mM KCl exhibited changes in Ca^{2+} transients upon depolarization. Ca^{2+} response is expressed as relative change in the fluorescence emission intensity above the normalized baseline (F/F_0). The plot is representative of three independent replicate experiments.

SEAP Assay. The production of human placental SEAP in cell-culture medium was assayed using a p-nitro phenyl phosphate-based light-absorbance time-course method as described previously (22, 43). Briefly, 120 μL of substrate solution [100 μL of 2× SEAP assay buffer including 20 mM homoarginine, 1 mM $MgCl_2$, 21% (wt/vol) diethanolamine, pH 9.8] and 20 μL of substrate solution containing 120 mM p-nitro phenyl phosphate was added to 80 μL of heat-deactivated (65 °C, 30 min) cell-culture supernatant, and the light absorbance was measured at 405 nm (37 °C) for 30 min using a Synergy H1 hybrid multimode microplate reader (BioTek Instruments, Inc.) using Gen5 software (version: 2.04).

Cell Viability Assay. HEK293 cells (1×10^4) were seeded into each well of a 96-well plate. At 24 h after culture, cells were exposed to FRL (1.5 mW/cm^2, 730 nm) or blue light (1.5 mW/cm^2, 465 nm) for 48 h, and cell viability was evaluated with the Cell Counting Kit-8 (Beyotime) according to the manufacturer's protocol. After treatment with CCK8 at 37 °C for 2 h, the absorbance was measured at 450 nm using a microplate reader (BioTek Instruments, Inc.).

qRT-PCR Analysis. Cells were harvested for total RNA isolation using an RNAiso Plus kit (catalog no. 9108; Takara) according to the manufacturer's instructions. A total of 1 μg RNA was reverse transcribed into cDNA using a PrimeScript RT Reagent Kit with the genomic DNA Eraser (catalog no. RR047; Takara) according to the manufacturer's protocol. qPCR analysis was performed on the QuantStudio 3 real-time PCR instrument (Thermo Fisher Scientific Inc.) using the SYBR Premix Ex Taq (catalog no. RR420; Takara) for detecting each target gene. Conditions for PCR amplifications were as follows: 95 °C for 10 min, 40 thermal cycles of 95 °C for 30 s, 60 °C for 30 s, and 72 °C for 30 s, and a final extension at 72 °C for 10 min. The qRT-PCR primers used in this study are listed in *SI Appendix*, Table S2. All samples were normalized to housekeeping *GAPDH* values, and the results are expressed as the relative mRNA level normalized to that in the dark using the standard ΔΔCt method.

Hollow Fiber Implants. Optogenetically engineered HEK293 cells (1×10^6) containing the FACE system or the blue light-inducible dCas9 transcription system CPTS 2.0 were seeded into a 2.5-cm semipermeable KrosFlo hollow fiber (Spectrum Laboratories Inc.), and both ends of the hollow fiber were heat-sealed using a Webster smooth needle holder. Two 2.5-cm hollow-fiber implants were s.c. implanted beneath the dorsal skin surface of each anesthetized mouse.

Mouse Experiments. The experiments involving animals were approved by the East China Normal University (ECNU) Animal Care and Use Committee and in direct accordance with the Ministry of Science and Technology of the People's Republic of China on Animal Care guidelines. The protocol (protocol ID: m20150304) was approved by the ECNU Animal Care and Use Committee. For hollow-fiber implantation experiments, the mice were randomly divided into four groups. The hollow fiber containing optogenetically engineered HEK293 cells was s.c. implanted into the shaved back skin of 12-wk-old male C57BL/6J wild-type mice (ECNU Laboratory Animal Center). Beginning 1 h after implantation, the mice were illuminated by FRL or blue light (5 mW/cm^2) for 2 h each day. The control mice were kept in the dark. The HEK293 cells were collected from the hollow fibers at 48 h after implantation for qRT-PCR analysis. For plasmid electroporation into mouse muscles, C57BL/6J male 4-wk-old wild-type mice were randomly divided into five groups with five mice in each group. Four experimental groups were electroporated with 40 μg of plasmids with the FACE system or CPTS 2.0; the remaining control group was electroporated with only saline. The tibialis posterior muscles of the mice were surgically exposed and electroporated with a total of 40 μg of plasmids for *Lama1* (FACE: 14.45 μg pWS46, 14.45 μg pGY32, 3.7 μg pGY102, and 7.4 μg pGY174 or CPTS 2.0: 13.3 μg pWS303, 13.3 μg pWS304, and 13.4 μg pGY174) or 40 μg of plasmids for *Fst* (FACE: 14.45 μg pWS46, 14.45 μg pGY32, 3.7 μg pGY102, and 7.4 μg pGY177 or CPTS 2.0: 13.3 μg pWS303, 13.3 μg pWS304, and 13.4 μg pGY177). The muscle was electroporated using the TERESA-EPT-I drug-delivery device (Shanghai Teresa Healthcare Sci-Tech Co., Ltd.) with the following parameters: voltage, 60 V; pulse width, 50 ms; frequency, 1 Hz. Beginning 18 h after electroporation, the mice were illuminated by FRL or blue light (10 mW/cm^2) for 4 h each day; control mice were kept in the dark. At 48 h after the first illumination, the mice in each group were killed, and the muscular tissues were collected for qRT-PCR analysis.

Lentivirus Production. HEK293 cells (5×10^6) were plated into a 15-cm dish for 18 h before transfection and incubation for 6 h with 2,000 μL of a 3:1 PEI:DNA mixture (wt/wt) containing 13.6 μg of the vector-of-interest plasmid, 6.8 μg of pMD2.G (catalog no. 12259; Addgene), and 13.6 μg of psPAX2 (catalog no. 12260; Addgene). The virus-containing supernatant was harvested at 48 h posttransfection, filtered with a 0.45-μm PVDF filter (catalog no. 12913999; Pall Life Sciences), and stored at −80 °C.

Mouse iPSC Culture and Stable Cell-Line Generation. Mouse iPSCs were maintained on irradiated mouse embryonic fibroblast feeder cells in 0.1% (wt/vol) gelatin-coated dishes in Glasgow Minimum Essential Medium (catalog no. 11710-035; Gibco) supplemented with 15% (vol/vol) FBS (catalog no. 16000-044; Gibco), 1% (vol/vol) nonessential amino acids (catalog no. 11140-050; Gibco), 1×10^{-3} M GlutaMAX (catalog no. 35050-061; Gibco), 0.1×10^{-3} M β-mercaptoethanol (catalog no. M3148; Sigma), and 1,000 U/mL recombinant mouse leukemia inhibitory factor (LIF; catalog no. ESG1107; Millipore). The medium was changed daily. To generate stable iPSCs incorporating the FACE construct, $\sim 5 \times 10^5$ cells were nucleofected with 100 ng of pWS287 (ITR–P_{hCMV}–p65–VP64–NLS–BldD–pA–P_{hCMV}–BphS–pA–P_{mPGK}–PuroR–pA–ITR), 100 ng of pWS289 [ITR–P_{FRL1b}–FGTA4–pA–P_{mPGK}–ZeoR–pA–ITR; P_{FRL1b}: pA–$(whiG)_3$–$P_{hCMVmin}$; FGTA4: MS2–P65–HSF1–ITR], and 20 ng of the Sleeping Beauty transposase expression vector pCMV–T7–SB100 (P_{hCMV}–SB100X–pA) using the P3 Primary Cell 4D-Nucleofector X Kit S (Lonza) and the CG-104 program. Following electroporation, these cells were seeded into 24-well gelatin-coated cell-culture plates in the presence of 1 μg/mL puromycin and 100 μg/mL zeocin to select for a mixed population.

iPSC Transduction and Optogenetic Neural Induction. The stable transgenic iPSCs line with the FACE system was transduced with lentivirus containing dCas9 [pXS187 (LTR–P_{EF1a}–dCas9–p2A–Blast–LTR)] and two sgRNAs [pWS74 (LTR–P_{U6}–sgRNA1 (*NEUROG2*)–LTR) and pWS76 (LTR–P_{U6}–sgRNA2 (*NEUROG2*)–LTR)] targeting *NEUROG2* (*SI Appendix*, Table S3) at 1 d after seeding into 24-well gelatin-coated cell-culture plates in the presence of 1 μg/mL puromycin and 100 μg/mL zeocin. Transduced cells were incubated at 37 °C in 5% CO_2 under FRL light illumination for 6 h each day or in the dark. Fresh growth medium without LIF was changed daily for 8 d. In the last 4 d, 5×10^{-7} M of all-*trans* retinoic acid (catalog no. R2625; Sigma) was added to the medium. The cells were then analyzed by immunofluorescence staining and qRT-PCR.

Immunofluorescence Staining. Cells were fixed with 4% (wt/vol) paraformaldehyde for 15 min, permeabilized with 0.2% Triton X-100 for 15 min, and then blocked with 10% (vol/vol) goat serum in PBS for 30 min at room temperature. Subsequently, the cells were incubated for 1 h with the primary antibodies anti-beta III tubulin (catalog no. MMS-435P; BioLegend) or anti-neurofilament 200 (catalog no. N4142; Sigma), both at 1:500 dilution. After incubation with the primary antibodies, cells were washed three times with PBS (5 min each time) and then were incubated with the secondary antibodies rabbit anti-mouse Alexa Fluor 488 or goat anti-rabbit Cy3 (1:200; Jackson ImmunoResearch) for 1 h. After three 5-min washings with PBS, the cell nuclei were counterstained with DAPI (0.25 μg/mL; Molecular Probes) for 10 min and were imaged under a 20× objective on an inverted fluorescence microscope (Leica DMI8).

Calcium Ion Imaging. After differentiation, the putative neuronal cells were washed three times with 1× HBSS (catalog no.14175095; Gibco) and then were stained with 3 μM of the calcium indicator Fluo-4 AM loading solution (catalog no. F14201; Gibco) for 60 min at 37 °C. Excess dye solution was then removed from the dish, and the cells were finally washed three times with 1× HBSS. The cells were exposed to a 50-mM KCl solution before imaging with a Leica DMI8 Microscope. Time-lapse imaging was performed at an excitation wavelength of 488 nm for 5 min. The data were analyzed using the Leica LAS AF software.

Statistical Analysis. All data are expressed as the mean ± SD, with sample sizes indicated in the figure legends. All qualitative images presented are representative of at least two independent duplicate experiments. Statistical significance was analyzed by the Student's *t* test. Prism 5 software (version 5.01; GraphPad Software Inc.) was used for statistical analysis. No sample exclusion was carried out, nor was randomization or blinding utilized in this study.

ACKNOWLEDGMENTS. We thank Prof. Dr. Jiemin Wong (ECNU) for providing mouse iPSCs and Jianli Yin for construction of the sgRNA pool. This work was financially supported by National Natural Science Foundation of China (NSFC) Grant 31522017 for Outstanding Young Scientists; the National Key Research and Development Program of China, Stem Cell and Translational Research Grant 2016YFA0100300; NSFC Grants 31470834 and 31670869, Science and Technology Commission of Shanghai Municipality Grant 18JC1411000; and the Thousand Youth Talents Plan of China (H.Y.).

1. Cho SW, Kim S, Kim JM, Kim JS (2013) Targeted genome engineering in human cells with the Cas9 RNA-guided endonuclease. *Nat Biotechnol* 31:230–232.
2. Cong L, et al. (2013) Multiplex genome engineering using CRISPR/Cas systems. *Science* 339:819–823.
3. Mali P, et al. (2013) RNA-guided human genome engineering via Cas9. *Science* 339: 823–826.
4. Dominguez AA, Lim WA, Qi LS (2016) Beyond editing: Repurposing CRISPR-Cas9 for precision genome regulation and interrogation. *Nat Rev Mol Cell Biol* 17:5–15.
5. Qi LS, et al. (2013) Repurposing CRISPR as an RNA-guided platform for sequence-specific control of gene expression. *Cell* 152:1173–1183.
6. Mougiakos I, et al. (2017) Characterizing a thermostable Cas9 for bacterial genome editing and silencing. *Nat Commun* 8:1647.
7. Ousterout DG, et al. (2015) Multiplex CRISPR/Cas9-based genome editing for correction of dystrophin mutations that cause Duchenne muscular dystrophy. *Nat Commun* 6:6244.
8. Gilbert LA, et al. (2013) CRISPR-mediated modular RNA-guided regulation of transcription in eukaryotes. *Cell* 154:442–451.
9. Jiang W, Bikard D, Cox D, Zhang F, Marraffini LA (2013) RNA-guided editing of bacterial genomes using CRISPR-Cas systems. *Nat Biotechnol* 31:233–239.
10. Hsu PD, Lander ES, Zhang F (2014) Development and applications of CRISPR-Cas9 for genome engineering. *Cell* 157:1262–1278.
11. Ran FA, et al. (2015) In vivo genome editing using Staphylococcus aureus Cas9. *Nature* 520:186–191.
12. Konermann S, et al. (2015) Genome-scale transcriptional activation by an engineered CRISPR-Cas9 complex. *Nature* 517:583–588.
13. Liu P, Chen M, Liu Y, Qi LS, Ding S (2018) CRISPR-based chromatin remodeling of the endogenous Oct4 or Sox2 locus enables reprogramming to pluripotency. *Cell Stem Cell* 22:252–261.e4.
14. Liao HK, et al. (2017) In vivo target gene activation via CRISPR/Cas9-mediated trans-epigenetic modulation. *Cell* 171:1495–1507.e1415.
15. Konermann S, et al. (2013) Optical control of mammalian endogenous transcription and epigenetic states. *Nature* 500:472–476.
16. Nihongaki Y, Kawano F, Nakajima T, Sato M (2015) Photoactivatable CRISPR-Cas9 for optogenetic genome editing. *Nat Biotechnol* 33:755–760.
17. Hemphill J, Borchardt EK, Brown K, Asokan A, Deiters A (2015) Optical control of CRISPR/Cas9 gene editing. *J Am Chem Soc* 137:5642–5645.
18. Polstein LR, Gersbach CA (2015) A light-inducible CRISPR-Cas9 system for control of endogenous gene activation. *Nat Chem Biol* 11:198–200.
19. Jain PK, et al. (2016) Development of light-activated CRISPR using guide RNAs with photocleavable protectors. *Angew Chem Int Ed Engl* 55:12440–12444.
20. Nihongaki Y, et al. (2017) CRISPR-Cas9-based photoactivatable transcription systems to induce neuronal differentiation. *Nat Methods* 14:963–966.
21. Müller K, et al. (2013) A red/far-red light-responsive bi-stable toggle switch to control gene expression in mammalian cells. *Nucleic Acids Res* 41:e77.
22. Shao J, et al. (2017) Smartphone-controlled optogenetically engineered cells enable semiautomatic glucose homeostasis in diabetic mice. *Sci Transl Med* 9:eaal2298.
23. Zalatan JG, et al. (2015) Engineering complex synthetic transcriptional programs with CRISPR RNA scaffolds. *Cell* 160:339–350.
24. Du D, et al. (2017) Genetic interaction mapping in mammalian cells using CRISPR interference. *Nat Methods* 14:577–580.
25. Gao Y, et al. (2016) Complex transcriptional modulation with orthogonal and inducible dCas9 regulators. *Nat Methods* 13:1043–1049.
26. Ryu MH, Gomelsky M (2014) Near-infrared light responsive synthetic c-di-GMP module for optogenetic applications. *ACS Synth Biol* 3:802–810.
27. Piatkevich KD, Subach FV, Verkhusha VV (2013) Engineering of bacterial phytochromes for near-infrared imaging, sensing, and light-control in mammals. *Chem Soc Rev* 42:3441–3452.
28. Tschowri N, et al. (2014) Tetrameric c-di-GMP mediates effective transcription factor dimerization to control Streptomyces development. *Cell* 158:1136–1147.
29. Bush MJ, Tschowri N, Schlimpert S, Flärdh K, Buttner MJ (2015) c-di-GMP signalling and the regulation of developmental transitions in streptomycetes. *Nat Rev Microbiol* 13:749–760.
30. Perrin A, Rousseau J, Tremblay JP (2017) Increased expression of laminin subunit alpha 1 chain by dCas9-VP160. *Mol Ther Nucleic Acids* 6:68–79.
31. Nicholas CR, et al. (2013) Functional maturation of hPSC-derived forebrain interneurons requires an extended timeline and mimics human neural development. *Cell Stem Cell* 12:573–586.
32. Samata B, et al. (2016) Purification of functional human ES and iPSC-derived midbrain dopaminergic progenitors using LRTM1. *Nat Commun* 7:13097.
33. Zhang Y, et al. (2013) Rapid single-step induction of functional neurons from human pluripotent stem cells. *Neuron* 78:785–798.
34. Berninger B, et al. (2007) Functional properties of neurons derived from in vitro reprogrammed postnatal astroglia. *J Neurosci* 27:8654–8664.
35. Chavez A, et al. (2015) Highly efficient Cas9-mediated transcriptional programming. *Nat Methods* 12:326–328.
36. Kennedy MJ, et al. (2010) Rapid blue-light-mediated induction of protein interactions in living cells. *Nat Methods* 7:973–975.
37. Chuong AS, et al. (2014) Noninvasive optical inhibition with a red-shifted microbial rhodopsin. *Nat Neurosci* 17:1123–1129.
38. Zetsche B, Volz SE, Zhang F (2015) A split-Cas9 architecture for inducible genome editing and transcription modulation. *Nat Biotechnol* 33:139–142.
39. Liu KI, et al. (2016) A chemical-inducible CRISPR-Cas9 system for rapid control of genome editing. *Nat Chem Biol* 12:980–987.
40. Simonsen JL, et al. (2002) Telomerase expression extends the proliferative life-span and maintains the osteogenic potential of human bone marrow stromal cells. *Nat Biotechnol* 20:592–596.
41. Saito H, Kubota M, Roberts RW, Chi Q, Matsunami H (2004) RTP family members induce functional expression of mammalian odorant receptors. *Cell* 119:679–691.
42. Wieland M, Ausländer D, Fussenegger M (2012) Engineering of ribozyme-based riboswitches for mammalian cells. *Methods* 56:351–357.
43. Xue S, et al. (2017) A synthetic-biology-inspired therapeutic strategy for targeting and treating hepatogenous diabetes. *Mol Ther* 25:443–455.